

Recent results and open questions on collective type phenomena from A-A to pp collisions

M. Petrovici, C. Andrei, I. Berceanu, A. Bercuci, A. Herghelegiu, A. Pop

National Institute for Physics and Nuclear Engineering (IFIN-HH), R-077125 Bucharest, Romania

Abstract. A review of the main results on the collective type expansion of the compressed and hot fireball formed in heavy ion collisions and some remarks to be considered when comparing multiplicity wise phenomena taking place in A-A, p-A and pp collisions, are followed by a discussion of the experimental results which seem to evidence collective type phenomena in pp collisions at $\sqrt{s} = 7$ TeV at high charged particle multiplicity. Correlations among the kinetic freeze-out temperature, the average transverse expansion velocity and its profile, as a function of centrality and multiplicity, extracted from the fits of experimental transverse momentum spectra with an expression inspired by hydrodynamical models, estimates on Bjorken energy densities and perspectives in selecting soft and close to azimuthal isotropic events in pp collisions are presented.

Keywords: SIS18, FOPI, RHIC, STAR, PHENIX, LHC, ALICE, CMS, PYTHIA, EPOS, light charged fragments, light charged hadrons, centrality, multiplicity, Glauber MC, highly central collisions, mid-central collisions, transverse momentum spectra, collective phenomena, azimuthal dependence, fireball shape dependence.

PACS: 25.75.-q, 25.75.Ld, 24.10.Nz, 24.10.Pa, 25.70.Pq, 05.20.-y, 05.90+m

1. INTRODUCTION

Strongly interacting matter in equilibrium can be characterized by two parameters, i.e. temperature T and baryon number density ρ_B or its conjugate variable, baryon chemical potential μ_B . It is well known by now that the basic property of Quantum Chromo-Dynamics (QCD), a non-Abelian gauge theory of quarks and gluons, is the asymptotic freedom, i.e. the QCD running coupling constant $\alpha_s(Q^2)$ becomes small for a momentum transfer Q much larger than the QCD intrinsic parameter Λ . Therefore, for $Q^2 \gg \Lambda^2$ a perturbative description of weakly interacting quarks and gluons becomes applicable. For $Q^2 \sim \Lambda^2$, quarks and gluons are strongly bound in clusters called hadrons. As $\Lambda_{QCD} \sim 200$ MeV, a phase transition from hadrons as strongly bound clusters of quarks and gluons to a deconfined state of matter formed by weakly interacting quarks and gluons is expected at temperature $T \sim \Lambda_{QCD} \sim O(10^{12}K)$ or baryon density $\rho_B \sim \Lambda_{QCD}^3 \sim 1 fm^{-3}$. In reality, the expectations based on QCD on the phase diagram of strongly interacting matter are more complex [1], as it is shown in Fig. 1. Besides the local gauge symmetry which is exact in the limit of vanishing quark masses, Chiral models predict the existence of a critical point E. For realistic u, d and s quark masses the Chiral transition becomes a first order transition for $\mu_B > \mu_E$ and a cross over for $\mu_B < \mu_E$. There are also predictions for another critical point F, at low T and high μ_B (μ_F, T_F). Below this point, for the cold QCD matter with three degenerate flavors, there is no border between superfluid nuclear matter and superconducting quark matter. The large N_c limit of QCD predicts a suppression of the quark loops relative to the gluon contribution [2, 3], an increase in the baryon number density at μ_B larger than the lowest baryon mass M_B being expected. This cold and dense matter was called quarkyonic matter [4]. Therefore, in the large N_c limit of QCD, the phase diagram has three regions, i.e. confined, deconfined and quarkyonic, separated by first order phase transitions.

The temperature T and chemical potential μ_B can be extracted in the framework of statistical models, which assume a gas of mesons, baryons and resonances in thermal equilibrium, by fitting the yield ratios at different collision energies. The extracted T and μ_B clusterize along a curve in the $T - \mu_B$ phase space. Along this line, which is not associated to any phase space boundaries, the thermal degrees of freedom are dominated by mesons for $\mu_B \ll M_N$ while at higher μ_B more baryons are excited. This suggests that there is a transitional change at the point (T_H, μ_H) where the role of baryons in thermodynamics surpasses that of mesons. According to statistical models this is located in the region of $\mu_H = 350 - 400$ MeV and $T_H = 150 - 160$ MeV. To what extent such a point is the correspondent of the triple point for finite N_c [5] is still under debate. In nature, according to the Big Bang cosmology, matter composed of quarks and gluons, characterized by negligible baryon chemical potential and high temperature, existed at a few microseconds after the Big Bang while the core of neutron stars could be the place where QCD matter at low temperature could exist. To what extent such states of matter could be produced and studied in the terrestrial laboratories is a fascinating

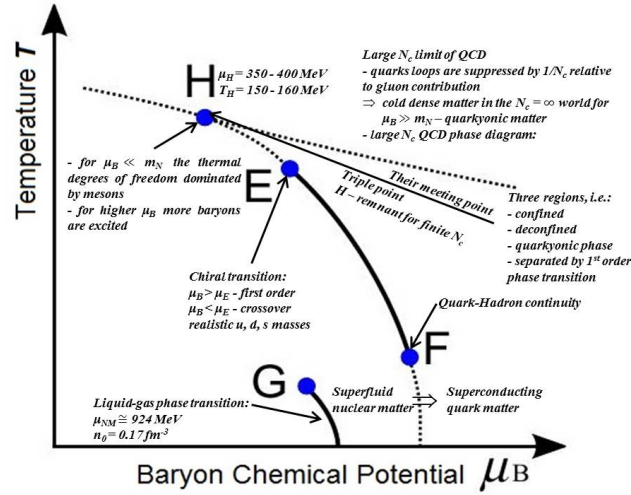


FIGURE 1. QCD expectations on critical points, triple point and phase transitions of the strongly interacting matter phase diagram [1].

question. By colliding heavy ions at relativistic and ultra-relativistic energies, transient pieces of matter at densities and temperatures discussed above can be produced. However, a few aspects which have to be considered from the very beginning are worth to be mentioned, i.e. even in the case of colliding the heaviest nuclei, the size of the created system is rather small, its initial state is highly non-homogeneous and dynamical effects play a crucial role, the system being characterized by a violent evolution. All these considerations have to be taken into account when trying to reconstruct detailed information on the dynamics and properties of each step of the evolution following the initial phase of the collision, from the particles and electromagnetic radiation reaching the detectors. At ultra-relativistic energies, even the hadrons become rather complex objects. A free hadron could be considered in each moment as a cloud of quasireal partons belonging to a cascade whose density, seen by a parton of a similar cascade from the colliding partner, increases with the energy being expected to reach a saturation at very high energy [6]. If a parton of a cascade meets on its way a parton of the colliding partner, interacts with it, the whole cascade changes, its coherence is broken, the partons cannot assembly back and they continue to live and decay in secondary hadrons and last but not least the struck cascade could interact with the others. Such multiparton interactions and rescatterings could contribute to a large energy transfer in a collision volume of proton size, easily reaching the deconfinement conditions. If this is the case and considering that the mean free path of the constituents in a deconfined medium is of the order of 0.2 - 0.3 fm, a close to equilibrium deconfined initial state could be expected in very high energy pp collisions. Therefore, quite probable at such energies, a piece of matter of proton size, with a radius of few times larger than the mean free path, expands hydrodynamically once the energy transfer is significantly large, i.e. low impact parameter - high charged particle multiplicity.

A review of the main results on the collective type expansion of the compressed and hot fireball formed in heavy ion collisions starting from SIS18 energies up to the highest one of $\sqrt{s_{NN}} = 2.76$ TeV at LHC is presented in Section 2. Section 3 is dedicated to some considerations on the differences one has to take into account in comparing multiplicity wise phenomena taking place in A-A, p-A and pp collisions. Experimental evidence on similar trends in the shape of transverse momentum (p_T) spectra of identified charged hadrons and their ratios in Pb-Pb at $\sqrt{s_{NN}} = 2.76$ TeV and p-Pb at $\sqrt{s_{NN}} = 5.02$ TeV collisions as a function of centrality and multiplicity classes, respectively and in pp collisions at $\sqrt{s} = 7$ TeV as a function of charged particle multiplicity are discussed in Section 4. In the same section, correlations among the kinetic freeze-out temperature, the average transverse expansion velocity and its profile, as a function of centrality and multiplicity, extracted from the fits of experimental p_T spectra with an expression inspired by hydrodynamical models are presented. Estimates on the Bjorken energy density and perspectives in selecting soft and close to azimuthal isotropic events in pp collisions are also included in this section. The conclusions are presented in Section 5.

2. $\langle \beta_T \rangle, T_{kin}, T_{ch}$ - COLLISION ENERGY DEPENDENCE

Detailed studies of collective type expansion of the fireball formed in heavy ion collisions as a function of the mass of the colliding nuclei and polar angle for highly central collisions [7, 8] evidenced a systematic enhancement of collective expansion going from 90 A·MeV to 400 A·MeV incident lab energy and from Ni+Ni to Au+Au. As can be followed in Fig. 2, this conclusion is based on the analysis performed around 90° polar angles in the center of mass system. In the forward direction, where Corona effects and fluctuations in the selected collision geometry play an important role and the average number of collisions suffered by the nucleons emitted in that direction is reduced, the extracted " E_{coll} " is artificially larger and its dependence on the mass of the colliding system is washed out.

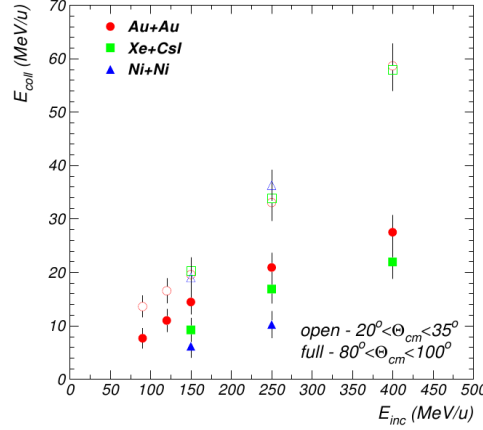


FIGURE 2. Collective energy per nucleon as a function of incident energy for three symmetric systems and highly central collisions (70 mb geometrical cross section) for $20^\circ < \theta_{cm} < 35^\circ$ (open symbols) and $80^\circ < \theta_{cm} < 100^\circ$ (full symbols) [7].

Under the assumption of a linear dependence of the expansion velocity as a function of the position in the fireball, which seems to be a rather good approximation at SIS18 energies [9], the average transverse expansion velocity can be obtained from the average collective energy per nucleon. At higher energies, the average transverse expansion velocity and kinetic freeze-out temperature were obtained as parameters of expressions inspired by hydrodynamical models [10] used to fit the experimental transverse momentum spectra of different reaction products:

$$E \frac{d^3N}{dp^3} \sim f(p_t) = \int_0^R m_T K_1(m_T \cosh \rho / T_{fo}) I_0(p_T \sinh \rho / T_{fo}) r dr \quad (1)$$

where $m_T = \sqrt{m^2 + p_T^2}$; $\beta_r(r) = \beta_s (\frac{r}{R})^n$; $\rho = \tanh^{-1} \beta_r$. A compilation in terms of the average transverse expansion velocity ($\langle \beta_T \rangle$) and the kinetic freeze-out temperature (T_{kin}) extracted using the above mentioned procedures and of the chemical freeze-out temperature extracted from fits of yield ratios using statistical model expressions for heavy ion central collisions can be followed in Fig. 3. Similar representations could be done as a function of baryon chemical potential μ_B [11]. As can be seen in Fig. 3, the average transverse expansion velocity and kinetic freeze-out temperature increase steeply to $\sim 50\%$ of the speed of light and 120 MeV, respectively, up to $\sqrt{s_{NN}} \sim 8$ GeV ($\mu_B = 400 - 500$ MeV) followed by a plateau up to $\sqrt{s_{NN}} \sim 20$ GeV ($\mu_B \sim 200$ MeV) and 40 GeV ($\mu_B \sim 100$ MeV), respectively. At higher collision energies a smooth logarithmic increase of the average transverse expansion velocity and decrease of freeze-out temperature up to the LHC energy is evidenced, the expectations for LHC based on the extrapolation of the results obtained at lower energies being confirmed. The chemical freeze-out temperature increases up to $\sqrt{s_{NN}} \sim 20$ GeV and remains rather constant at a value of $\cong 160 - 165$ MeV. As far as concerns the dependence of the expansion as a function of centrality, starting from $N_{part} \sim 100$, $\langle \beta_T \rangle$ shows a very weak dependence on N_{part} starting from 400 MeV up to the LHC energy. For mid-central collisions at low energies [16] and also at 200 GeV [17] it was evidenced that for the same N_{part} the more rounded objects expand more violently than the almond shape ones if the analysis is done at 90° relative to the reaction plane. In-plane, the results are quite different. While at 200 GeV there is no difference between the expansion of fireballs corresponding to different symmetric colliding systems for a given N_{part} [17], at much lower energies where there is a balance between the expansion time and passing time of the spectators and the Lorentz contraction is rather negligible, the shadowing effects of the spectators play an important role and the observed in-plane expansion is lower for the heavier symmetric combination for a given N_{part} [16].

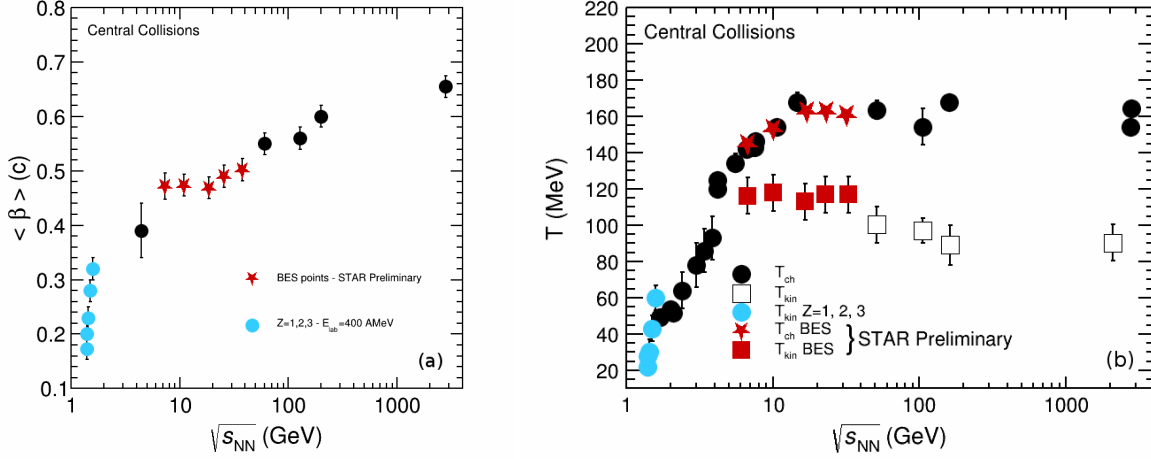


FIGURE 3. (a) $\langle \beta_T \rangle$ as a function of $\sqrt{s_{NN}}$ for heavy ion central collisions [8, 11, 12, 13, 14]; (b) Chemical (T_{ch}) and kinetic freeze-out temperatures for heavy-ion central collisions as a function of the collision energy $\sqrt{s_{NN}}$ [11, 12, 13, 14, 15].

3. COLLISION GEOMETRY IN A-A, p-A AND pp SYSTEMS

The amount of energy density of the system produced in heavy ion collisions depends on the amount of overlapping matter, therefore on the impact parameter. From the fits of the experimental charged particle multiplicity distributions based on Glauber Monte Carlo estimates of the number of ancestors and negative binomial distributions for charged particle multiplicity in nucleon-nucleon interactions [18], a rather good impact parameter selection can be achieved in A-A collisions. The situation becomes delicate for p-A collisions where the correlation between the number of wounded nucleons and the impact parameter becomes rather broad relative to A-A. What about the pp case?

Within the geometrical model approach of particle production [19, 20] and $\sigma_{in}(b,s)=1-\exp(-kO(b))$ where $O(b)$ is the overlap function resulting from spherically symmetric double Gaussian distributions of the hadronic matter inside the colliding protons, like in PYTHIA, with parameters fixed in order to get the best agreement with the experiment [21], the charged particle multiplicity - impact parameter correlation is obtained by solving the following integral equation:

$$\int_0^{w(b)} \psi(w)dw = \frac{1}{\sigma} \int_b^\infty d^2b \sigma(b) \quad (2)$$

where $w(b)=\bar{n}(b)/\bar{N}$, $\bar{N}P(n)=\psi(z,\bar{N})$, $z=n/\bar{N}$. In order to obtain $\psi(w)$, the charged particle multiplicity distribution [22] represented in the KNO variable $z = N_{ch}/\bar{N}^{MB}$ was used. The result is presented in Fig. 4(a) with black points. As a cross-check, the overlap function obtained by a recent parametrization [23] (Fig. 4(b)) which reproduces the elastic differential cross section of pp scattering at 7 TeV [24] was also used. The result is represented in Fig. 4(a) with green symbols. These results show that at high charged particle multiplicities, i.e. 5-6 times larger than the mean value corresponding to the minimum bias multiplicity distribution, events close to central pp collisions could be selected. Using the Glauber Monte Carlo approach where the black disk approximation for nucleon-nucleon cross section is replaced by the above ansatz for $\sigma_{in}(b,s)$ the average distance between colliding nucleons at different centralities for Pb-Pb at 2.76 TeV and p-Pb at 5.02 TeV, measured at LHC, can be estimated. The results for $3 \cdot 10^4$ events for each of the two systems are presented in Fig. 5. The distributions are normalized to the number of events.

In Pb-Pb collisions at all three centralities represented in Fig. 5(a), the percentage of events for which the average distance between the wounded nucleons is smaller than 1.1 fm is rather low. In the p-Pb case (Fig. 5(b)) there are events in which the average distance goes down to 0.5 fm. However, there is no possibility to select such events based on charged particle multiplicity, the interplay between the collision geometry and the nucleon-nucleon impact parameter contributions to the charged particle multiplicity being rather complex. Therefore, the only way to study phenomena as a function of impact parameter at the nucleonic level is the analysis of pp collisions as a function of charged particle multiplicity and any direct comparison between the three systems in terms of charged particle multiplicity has to be carefully considered. For a large overlap in a pp collision at high energy, the probability of multi-interactions among

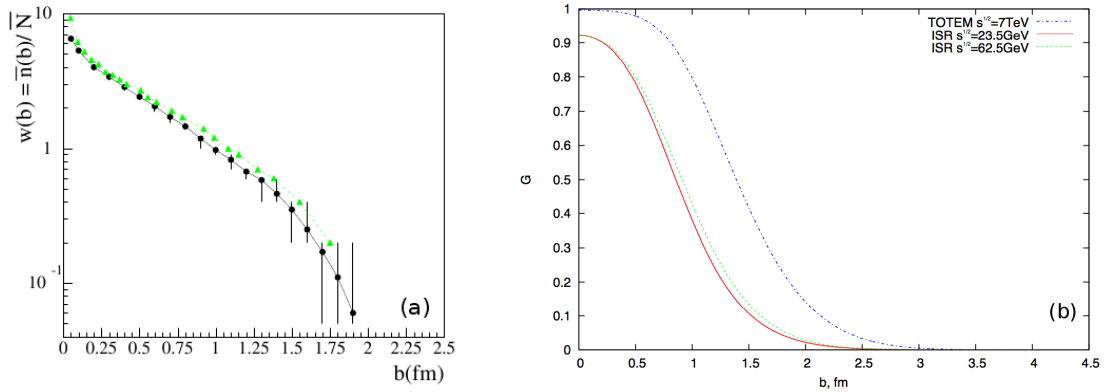


FIGURE 4. (a) Charged particle multiplicity - impact parameter correlation based on: PYTHIA-like overlap function (black symbols) and overlap function from [23] (green symbols); (b) Overlap function: PYTHIA-like and from [23].

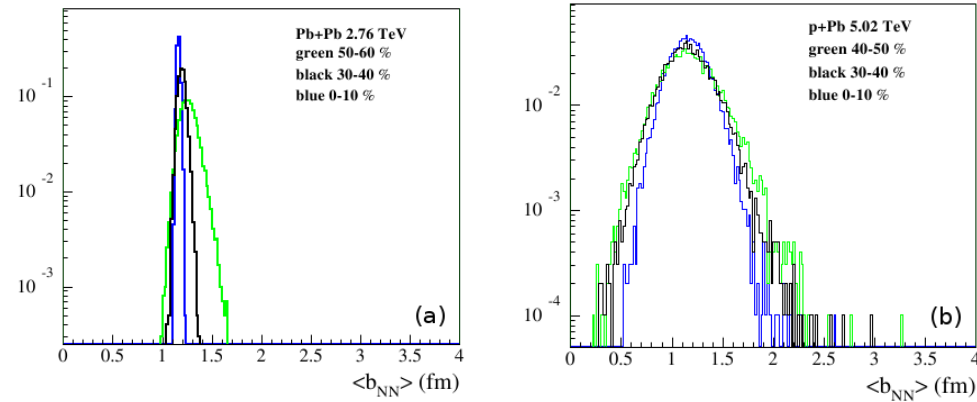


FIGURE 5. (a) The average distance between colliding nucleons at different centralities for Pb-Pb at 2.76 TeV using $3 \cdot 10^4$ events; (b) The average distance between colliding nucleons at different centralities for p-Pb at 5.02 TeV using $3 \cdot 10^4$ events.

the quasi-real cascades of partons and rescattering of the struck cascades increases and could contribute to a large energy transfer in a small collision volume of proton size. The energy density easily reaches the deconfinement value and considering the mean free path of the constituents of the deconfined phase, thermalization cannot be excluded. If this is the case, such an initial state, thermalized and of extremely high energy density, will follow a collective type expansion [25, 26, 27, 28] which can be evidenced experimentally by analyzing the same observables as the ones presented above for A-A collisions.

4. TRANSVERSE MOMENTUM SPECTRA OF IDENTIFIED CHARGED HADRONS AND THEIR RATIOS IN pp COLLISIONS AT $\sqrt{s} = 7$ TeV AS A FUNCTION OF CHARGED PARTICLE MULTIPLICITY

The ALICE Collaboration has recently presented detailed results on transverse momentum spectra of π^+ , K^+ and p measured at LHC in pp collisions at $\sqrt{s} = 7$ TeV as a function of charged particle multiplicity [29]. The charged particle multiplicity was measured in the central pseudorapidity region $|\eta| \leq 0.8$ and the analysis was done in a narrower range of rapidity $|y| \leq 0.5$. The p_T spectra (Fig. 6(a) - upper row) were analyzed from 0.2 GeV/c, 0.3 GeV/c and 0.5 GeV/c up to 2.6 GeV/c, 1.4 GeV/c and 2.6 GeV/c for π^+ , K^+ and p respectively and in eight bins of multiplicity up to ~ 50 measured charged particle multiplicity density per unit of pseudorapidity. A clear depletion in the low p_T region of

the spectra ratios to MB as a function of charged particle multiplicity can be seen in Fig. 6(a) - bottom row. The ratio of the p_T spectra of K^+ and protons relative to π^+ and protons relative to K^+ for the second and the sixth multiplicity bins are represented in the upper row and their ratios to the values corresponding to MB case in the bottom row of Fig. 6(b). At large multiplicities heavier particles, i.e. protons relative to K^+ and π^+ and K^+ relative to π^+ , are pushed towards large p_T values, in other words depleted in the low p_T range. Such a trend, evidenced in Pb-Pb collisions at 2.76 TeV was explained by the existence of a common boost due to collective expansion [14]. Qualitatively, a similar trend is observed in the EPOS-LHC model in which a collective hadronization process is included in the pp scattering [30]. This trend was also evidenced recently in p-Pb collisions at 5.02 TeV for central collisions [31]. As it was presented in the first section, information on collective type dynamics in heavy ion collisions from the fits of experimental transverse momentum spectra using expressions inspired by hydrodynamical models [10] was obtained. The result of these fits done simultaneously on π^+ , K^+ and p spectra, in terms of $T_{kin} - \langle \beta_T \rangle$ correlation as a function of charged particle multiplicity and comparison with the results obtained for Pb-Pb and p-Pb as a function of centrality and multiplicity classes, respectively, are presented in Fig. 7(a) [29]. One could conclude that for pp collisions at 7 TeV, the $T_{kin} - \langle \beta_T \rangle$ correlation as a function of charged particle multiplicity has a trend rather similar with the one observed in heavy ion collisions, i.e. the freeze-out kinetic temperature decreases and the average transverse expansion velocity increases with charged particle multiplicity (pp) or increasing centrality (A-A). However, there is a quantitative difference between pp and A-A collisions, i.e. T_{kin} is systematically lower and $\langle \beta_T \rangle$ systematically larger than the pp values, the difference increasing towards higher centralities. Within the error bars, the results for p-Pb at 5.02 TeV are the same with the ones evidenced in pp. Such a correlation is not reproduced by PYTHIA for the pp case. Including the color reconnection mechanism [32] it seems that the model starts to show a similar trend but with values of T_{kin} about 40 MeV lower. On Fig. 7(b) a similar plot [11] is shown, including all energies measured at RHIC [11] and Pb-Pb at 2.76 TeV [14].

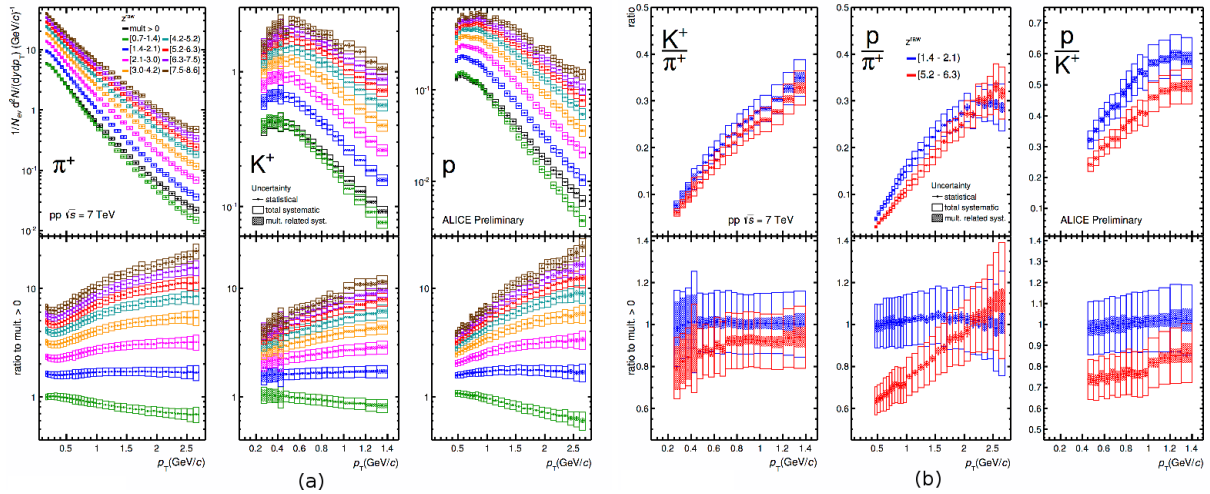


FIGURE 6. (a) p_T spectra and their ratio to the corresponding MB spectra, for π^+ , K^+ and p for eight charged particle multiplicity bins for pp collisions at $\sqrt{s} = 7$ TeV measured by ALICE at LHC. (b) p_T dependent yield ratios and their ratios to the MB case for two multiplicity bins [29].

Another aspect worth to be mentioned is the correlation between the expansion profile $\langle n \rangle$ and $\langle \beta_T \rangle$. This correlation is presented in Fig. 8(a) [29]. It is clearly seen that all three systems follow exactly the same correlation. Towards the highest multiplicity in the pp case, the expansion velocity becomes linear as a function of position within the fireball. The $\langle n \rangle - 1/T_{kin}$ correlation (Fig. 8(b)) obtained using PYTHIA results is completely different than the experimental one. Using EPOS3 estimates of the mean transverse momentum ($\langle p_T \rangle$) for π^+ , K^+ and p as a function of multiplicity [33], the relative yields measured by the CMS Collaboration in pp collisions at 7 TeV [34] and the impact parameter-charged particle multiplicity correlation presented in Fig. 4(a), a rough estimate of the Bjorken energy density times the formation time, i.e. $\varepsilon_{Bj} \cdot \tau$, was made for the highest charged particle multiplicity measured by CMS within the pseudorapidity range $|\eta| \leq 2.4$. The obtained value is $\simeq 10$ GeV/fm². Based on PYTHIA simulations, the largest multiplicity bin measured by CMS would correspond to the fifth multiplicity bin measured by ALICE [29]. Therefore, quite probable at the largest multiplicity bin measured by ALICE, the Bjorken energy density is similar with the value of ~ 17.5 GeV/fm² estimated for the highest centrality (0-5%) Pb-Pb collisions at 2.76 TeV.

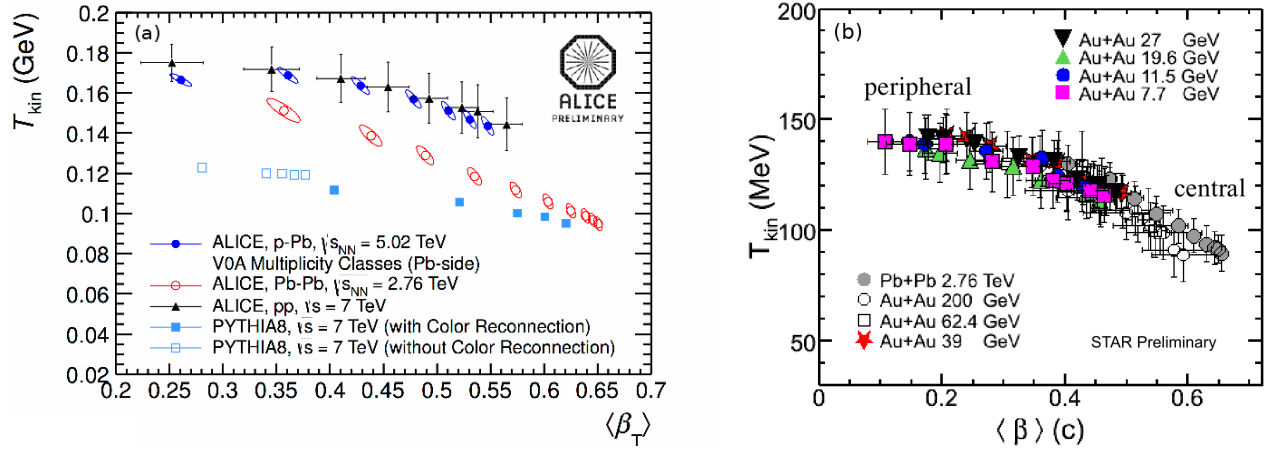


FIGURE 7. (a) $T_{kin} - \langle \beta_T \rangle$ correlation as a function of multiplicity, multiplicity classes and centrality for pp ($\sqrt{s} = 7$ TeV), p-Pb ($\sqrt{s_{NN}} = 5.02$ TeV) and Pb-Pb ($\sqrt{s_{NN}} = 2.76$ TeV), respectively [29, 31]; (b) $T_{kin} - \langle \beta_T \rangle$ correlation as a function of centrality for Au+Au at RHIC energies [11] and Pb-Pb [14].

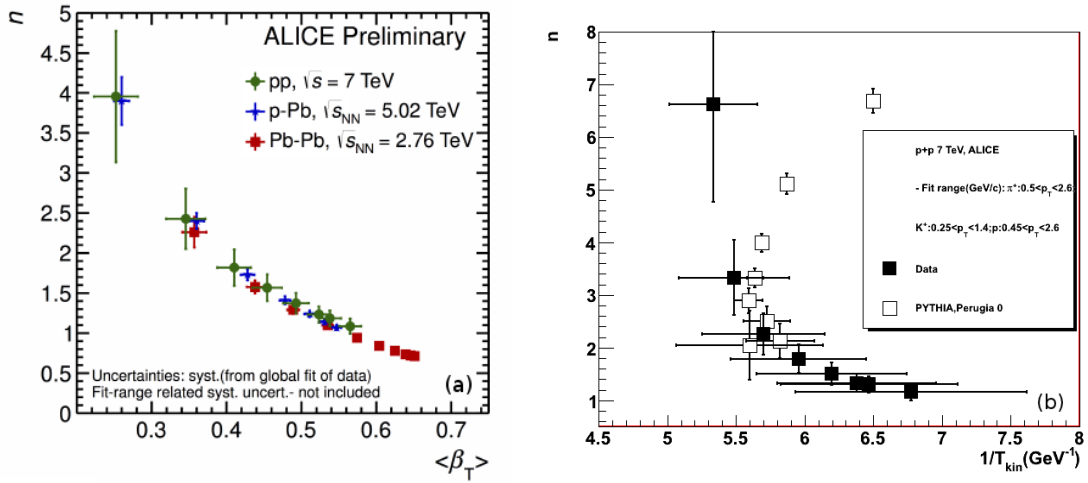


FIGURE 8. (a) $n - \langle \beta_T \rangle$ correlation as a function of charged particle multiplicity in pp at 7 TeV and centrality and multiplicity classes in Pb-Pb at 2.76 TeV and p-Pb at 5.02 TeV, respectively [29]; (b) $n - 1/T_{kin}$ correlation as a function of charged particle multiplicity in pp at 7 TeV; data - full symbols, PYTHIA - open symbols.

Although these preliminary results seem to indicate that for events with high charged particle multiplicity in pp collisions at 7 TeV collective type phenomena show up, the experimental and theoretical efforts to understand the physics behind the evidenced trends remain to be done. On the experimental side one important aspect is to discriminate between hard and soft processes, jets influence on the analysis based only on multiplicity selection not being negligible. Studies along the possibility to select events close to azimuthal isotropy using global event shape observables like Directivity, Sphericity, Thrust or Fox-Wolfram moments have shown their performance in selecting soft, nearly azimuthal isotropic events [35, 36]. As an example, the correlations between charged particle multiplicity and Directivity, Thrust and Sphericity, based on PYTHIA events for pp at 7 TeV, are shown in Fig. 9. Although the correlations are rather good, it is clearly seen that even at the highest multiplicities the global event shape variables have a rather broad distribution. Therefore, a two dimensional condition in multiplicity and different event shape variables could significantly contribute in selecting events with specific azimuthal distributions for a given multiplicity. An example in this respect is presented in Fig. 9(d) where an azimuthal isotropic event was selected based on Fox-Wolfram

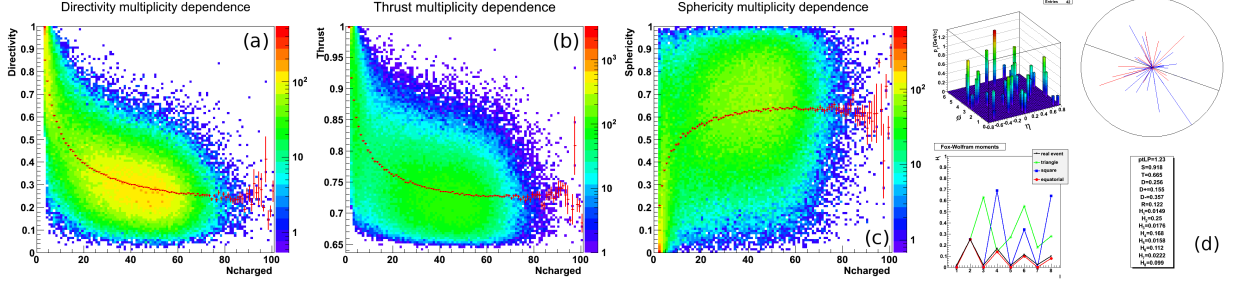


FIGURE 9. (a) Directivity - multiplicity correlation for PYTHIA pp collisions at 7 TeV [35, 36]; (b) Thrust - multiplicity correlation for PYTHIA pp collisions at 7 TeV [36]; (c) Sphericity - multiplicity correlation for PYTHIA pp collisions at 7 TeV [36]; (d) An example of selection performance of an azimuthal isotropic event using Fox-Wolfram moments [36].

moments. The two-dimensional distribution of particles for such an event in η - ϕ and p_x - p_y confirms the expectation.

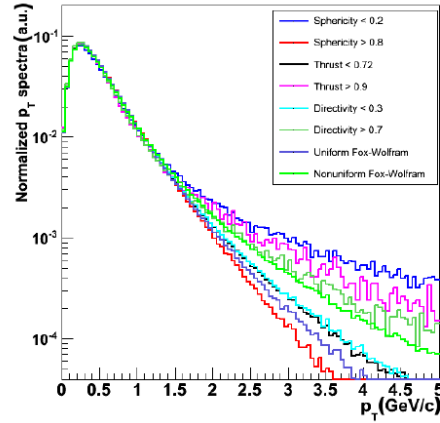


FIGURE 10. PYTHIA p_T spectra of positive charged particles for MB events for jet-like and close to azimuthal isotropic events selected by different event shape global variables [36].

An example of the influence of such selections on the p_T spectra of charged particles obtained with PYTHIA, is shown in Fig. 10. In general, selecting events close to isotropy based on the four global event shape variables reduces significantly the power law tail of the p_T spectra.

5. CONCLUSIONS

Evidence for collective type expansion of the hot and compressed fireball produced in heavy ion collisions is presented for all collision energies, starting from below $\sqrt{s_{NN}} = 1.5$ GeV up to 2.76 TeV. The expansion velocity increases steeply to about half of the speed of light up to $\sqrt{s_{NN}} = 8$ GeV, corresponding to a baryonic chemical potential where the thermal degrees of freedom start to be dominated by mesons. Above this value, the expansion velocity shows a plateau up to $\sqrt{s_{NN}} \sim 20$ GeV when it starts to increase again logarithmically with a much lower slope up to the LHC energy. The kinetic freeze-out temperature follows a similar trend up to $\sqrt{s_{NN}} \sim 40$ GeV beyond which it slowly decreases, the system being cooled down during the expansion. The chemical freeze-out temperature increases up to $\sqrt{s_{NN}} \sim 20$ GeV and remains rather constant at a value of $\sim 160 - 165$ MeV. At a given number of participating nucleons, the almond shape fireballs expand less violently along the major axis than the round shape ones. Above $N_{part} \sim 100$, $\langle \beta_T \rangle$ shows a very weak dependence on N_{part} for all collision energies.

Transverse momentum distributions and their ratios for π^+ , K^+ and p at mid-rapidity ($|\eta| < 0.5$) for different charged particle multiplicity bins in pp collisions at $\sqrt{s} = 7$ TeV show an enhanced depletion of heavier species relative to the lighter ones in the low p_T region with increasing charged particle multiplicity. The quality of simultaneous fits of the experimental spectra using the Boltzmann-Gibbs Blast Wave expression and the dynamics of the extracted kinetic

freeze out temperature, average transverse expansion velocity and its profile as a function of multiplicity are similar with those obtained in heavy ion collisions. Preliminary estimates of the Bjorken energy density for high multiplicity events indicate values close to the ones estimated for the central Pb-Pb collisions at $\sqrt{s_{NN}} = 2.76$ TeV. The selection of high multiplicity events close to azimuthal isotropy based on event shape global observables seems to be feasible. A direct comparison among pp, p-Pb and Pb-Pb based on charged particle multiplicity has to be taken with care. A factor two in the collision energy, soon available at LHC and the expected higher statistics will give access to extend these studies at heavy flavor hadrons and detailed comparisons with the results obtained in A-A collisions.

REFERENCES

1. K. Fukushima and T. Hatsuda. Rep. Prog. Phys., **74**:014001, 2011.
2. G. t' Hooft. Nucl. Phys., **B72**:461, 1974.
3. E. Witten. Nucl. Phys., **B160**:57, 1979.
4. L. McLerran and R.D. Pisarski. Nucl. Phys., **A796**:83, 207.
5. A. Andronic et al. Nucl. Phys., **A837**:65, 2010.
6. L.V. Gribov et al. Phys. Rep., **100**:1, 1983.
7. M. Petrovici. Proc. Int. Symp. Advances in Nucl.Phys., page 242, 2000.
8. M. Petrovici and A. Pop. *AIP Conf. Proc.*, **972**:98, 2008.
9. FOPI Collaboration" "M. Petrovici et al. "Phys. Rev. Lett.", **74**:5001, 1995.
10. E.Schnedermann et al. Phys. Rev. C, **48**:2462, 1993.
11. STAR Collaboration" "L. Kumar. "*Quark Matter 2014*".
12. E802 Collaboration C. Muntz for Experiment 866. arXiv:nucl-ex, **9806002**, 1998.
13. STAR Collaboration B. I. Abelev et al. Phys. Rev. C, **79**:034909, 2009.
14. ALICE Collaboration B. Abelev et al. Phys. Rev. C, **88**:044910, 2013.
15. G. Stoicea. PhD Thesis, Bucharest University, 2003.
16. FOPI Collaboration G. Stoicea et al. *Phys. Rev. Lett.*, **92**:072303, 2004.
17. PHENIX Collaboration" "M. Shimomura. "J. of Phys. Conf. Series", **270**:012041, 2011.
18. S. J. Sanders M. L. Miller, K. Reygers and P. Steinberg. Ann. Rev. Nucl. Part. Sci., **57**:205, 2007.
19. H. Moreno. Phys. Rev. D, **8**:268, 1973.
20. A.Bialas and E.Bialas. Acta Phys. Polonica, **B5**:373, 1974.
21. ATL-PHYS-PUB-2010-, **002**, 2010.
22. CMS Collaboration V. Khachatryan et al. JETP, **1101**:79, 2011.
23. M. Dremin et al. arXiv:hep-ph, **1306.5384**, 2013.
24. G. Antchev et al. Eur. Phys. Lett., **101**:21004, 2013.
25. L.D. Landau S. Z. Belenkji. Del Nuovo Cim., Suppl., **Vol.III,Serie X,No.1**:15, 1956.
26. G. A. Malekhin. Zh. Eksp. Teor. Fiz., **35**:1185, 1958.
27. L. Van Hove. Phys. Lett. B, **118**:138, 1982.
28. B. Andersson et al. Physica Scripta, **20**:10, 1979.
29. ALICE Collaboration C. Andrei et al. Nucl. Phys. A 20024, **S0375-9474(14)00251-6**:10.1016/j.nuclphysa.2014.08.002, Quark Matter 2014.
30. T. Pierog et al. arXiv:hep-ph, **1306.0121**, 2013.
31. ALICE Collaboration B. Abelev et al. Phys. Lett. B, **728**:25, 2014.
32. R.Corke and T. Sjostrand. JHEP, **1001**:35, 2010.
33. K. Werner et al. arXiv:nucl-th, **1312.1233**, 2013.
34. CMS Collaboration V. Khachatryan et al. Eur. Phys. J C, **72**:2164, 2012.
35. C. Andrei. PhD Thesis, Bucharest University, 2013.
36. A.Herghelegiu. PhD Thesis, Bucharest University, 2013.